JOURNAL OF MATERIALS SCIENCE **34** (1999) 2089–2102

Shear-induced crystallization of polypropylenes: effect of molecular weight

F. JAY, J.M. HAUDIN, B. MONASSE
Ecole des Mines de Paris, Centre de Mise en Forme des Matériaux, Unité Mixte de Recherche CNRS no. 7635, BP 207, 06904 Sophia Antipolis, France

The crystallization kinetics of three polypropylenes with different molecular weights was studied during shear under isothermal condition with a fibre pull-out device. Nucleation and growth under shear were observed and compared to static conditions. The crystalline growth rate was measured both in static condition and under shear. In static condition, the morphologies are α-phase spherulites and are formed from nuclei which are randomly distributed. Under shear α-phase morphologies are still observed but the nucleation density and the growth rate depend on the shear-rate. The nucleation density is strongly enhanced by shear and acts as the main factor on the overall kinetics. The growth rate increases with the shear-rate, but the basic growth mechanisms seem to be unmodified. β phase appears after shear during the relaxation of the orientation.

1. Introduction

Flow-induced crystallization is of great interest because it implies the possibility of controlling and predicting the final morphologies and properties of semi-crystalline polymers in current transformation processes like injection-molding or extrusion. Due to flow, polymer chains are oriented in the melt and can crystallize with morphologies different from those encountered under quiescent conditions (observation of shish-kebabs or row-nucleated structures rather than usual spherulites). Various devices able to apply shear have been built in order to study crystallization under or after shear [1–22]: parallel-plate [1–5], coaxial cylinders [6–11], rotational plate-plate [9, 12], biconical [13], fibre pull-out [14–21], die extrusion [22]. Many studies have been concerned with the measurement of the induction time of crystallization [1, 3, 7, 8, 13] because the onset of crystallization is relatively easy to characterize by an increase of the force or the transmitted torque. Some studies [8, 9, 11] have determined the fraction of transformed material versus time but few *in-situ* measurements concern the density of nuclei formed under shear and the growth rate of the subsequent morphologies [12]. More recent work on the crystallization of polypropylene induced by the displacement of a fibre [14–21] deal with the conditions of appearance of row-nucleated structures or cylindrites near the fibre, and with the type of crystalline phase encountered. These shear experiments must be compared with static ones where the type of fibre is recognized to act on surface nucleation and leads to a transcrystalline zone [23, 24]. The origin of crystallization under shear is discussed: strain-rate, shear-strain, shear-stress or residual stresses [3, 16, 18, 21, 25]. From shear experiments in a parallelepipedic duct [22], Janeschitz-Kriegl has recently proposed a model for shear-induced crystallization [22, 26]. It is based on the existence of "thread-like precursors" resulting from molecular orientation during flow.

Two of these apparatus have been applied in our laboratory, a plane-plane shear [4, 5] and a fibre pull-out device [5, 14, 15]. They make it possible to perform isothermal crystallizations after a rapid cooling, under an optical microscope. The appearance and development of crystalline morphologies can be observed during crystallization. They slightly differ by their performances. The plane-plane device allows us to shear the polymer melt at a constant shear-rate (up to $\dot{\gamma} = 30\,s^{-1}$), but the direct observation of the morphologies in the shear plane is not possible [4]. On the contrary, the fibre pull-out device allows us to observe the morphologies in the shear plane but the shear flow ($\dot{\gamma}$ up to $300\,s^{-1}$) is localized near the fibre and not constant [14]. A lot of experiments have been done with these apparatus on different polymers and under various conditions. The crystallizations have been studied under shear [4] or after application of a shear [5, 14, 15]. We have measured overall kinetics [5, 15], nucleation rate and density [5], and growth rates [4, 5] on polyethylene [4] and polypropylenes [5, 14, 15]. The overall crystallization kinetics is enhanced by shear whenever crystallization appears during shear [4] or after shear [5, 15]. The main mechanism responsible for the enhancement depends on the polymer: shear mainly affects the growth rate of polyethylene [4], the nucleation of polypropylene [5, 14, 15], and slightly its growth rate [5].

Up to now our crystallization experiments with the fibre pull-out device have been performed after shear, with three different polypropylenes [5, 14, 15]. The scope of the present paper is to measure the crystallization kinetics of polypropylenes with various molecular weights during shear experiments. The nucleation

and the growth rate of the subsequent morphologies will be studied as a function of molecular weight and shear-rate.

2. Experimental

The effect of shearing on crystallization was studied on three polypropylenes which mainly differ by their molecular weights. The morphologies and crystallization kinetics were characterized during shear. More precise analyses of morphologies and crystalline phases around the fibre were made from thin slices cut out of samples after crystallization. A new sample, with an identical preparation, was used for each crystallization experiment.

2.1. Materials

Three isotactic polypropylene homopolymers supplied by Borealis were used under the references A ($\bar{M}_n = 58\,900$ g/mol, $\bar{M}_w = 208\,000$ g/mol, $\bar{M}_w/\bar{M}_n = 3.5$, atactic % = 4.5), B ($\bar{M}_n = 53\,600$ g/mol, $\bar{M}_w = 268\,000$ g/mol, $\bar{M}_w/\bar{M}_n = 5$, atactic % = 3.8) and C ($\bar{M}_n = 77\,400$ g/mol, $\bar{M}_w = 377\,000$ g/mol, $\bar{M}_w/\bar{M}_n = 4.8$, atactic % = 2.3). These polymers mainly differ by their $\bar{M}_w$ molecular weights. Each individual glass fibre coated with an unsaturated polyester (diameter 17 μm, length 20 cm) was pulled out of a mesh of 100 identical fibres.

The viscosity η of the three polymers as a function of the frequency ω (0.05 rad $s^{-1} \leq \omega \leq$ 200 rad s^{-1}) was measured by Borealis with a Rheometrics RD-II rheometer at 190, 220 and 260 °C (Fig. 1). Above a critical shear-rate (20 s^{-1} for A, 10 s^{-1} for B and 8 s^{-1} for C at 190 °C), the polymer melt exhibits a shear-thinning behaviour, which can be described by a power law:

$$\eta = K\dot{\gamma}^{n-1} \quad (1)$$

where $\dot{\gamma}$ is the shear-rate, n is assumed to be constant, which is licit in the investigated shear-rate range, and K is temperature dependent. Its variation with temperature can be correctly fitted by an Arrhenius law, which gives access to an activation energy E_a. The rheological parameters K (190 °C), E_a and n depend on the polymer (Table I) and will be used for the mechanical analysis of crystallization under shear (see Section 4).

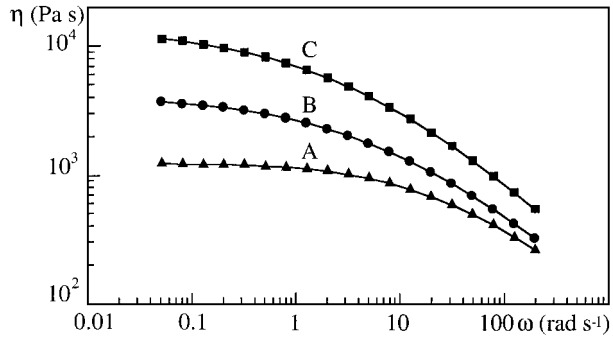

Figure 1 Viscosity of the three polypropylenes measured at 190 °C in dynamic experiments.

TABLE I Rheological parameters of the three polymers at 190 °C according to a power law with an Arrhenius thermal dependence of K. E_a is the activation energy

	Polymer A	Polymer B	Polymer C
K (Pa s^m)	2 224	4 311	12 247
E_a (J mol^{-1})	40 200	35 300	35 500
n	0.60	0.52	0.42

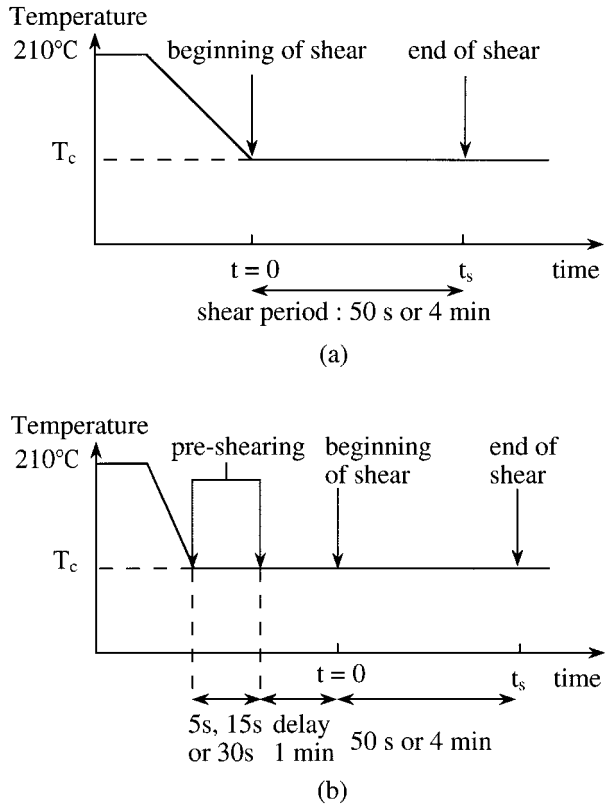

Figure 2 Experimental procedure for crystallization under shear: (a) standard procedure and (b) procedure with a pre-shearing applied on polymer A.

2.2. Shear apparatus and experimental method

These experiments consist in pulling a glass fibre in a molten polymer at the crystallization temperature after a heat treatment performed under static condition (Fig. 2). According to a method described previously [14], a two-step sample preparation was used to incorporate the fibre inside the polymer melt. Solid polypropylene films (200 μm thick) were prepared and the long glass fibre was partially sandwiched between two of these 3 cm-long films. This sample was then melted in the Mettler FP 52 hot stage at 210 °C between two glass slides and put under an optical microscope Reichert Zetopan-Pol with transmitted polarized light (Fig. 3). The spacing between the slides was controlled and was equal to 330 μm; the sample width was about 5 mm. This procedure ensures that the fibre is located in the middle of the polymer melt all along the sample. A thick specimen is necessary to approach the condition of a polymer flow around a fibre in a cylindrical medium, which is assumed in the model (see Section 4). The heat treatment at 210 °C during 5 min is

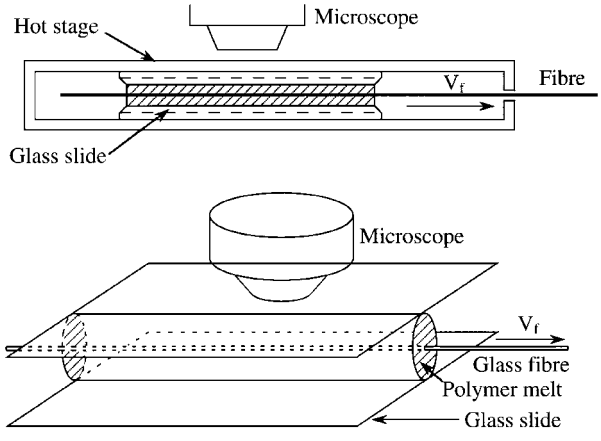

Figure 3 Scheme of the fibre pull-out device.

necessary to erase any previous thermo-mechanical history inside the sample. Then, the specimen was cooled at 10 °C min^{-1} down to the isothermal crystallization temperature T_c. These thermal treatments were done without any movement of the fibre and with a microscopical observation in order to ensure that the crystallization did not appear before the application of shear under isothermal condition. When the crystallization temperature was reached, the fibre was displaced at a constant speed V_f. The morphologies growing from or in the vicinity of the glass fibre surface were observed and photographed during the fibre displacement, at constant time intervals. Likewise, as a reference, isothermal crystallization experiments in static condition were performed in the same hot stage with the fibre in place but without any displacement.

The Mettler FP 52 hot stage was calibrated in temperature with benzoic acid (melting temperature T_m = 122.35 °C) under isothermal condition. The calibration and the experiments in the hot stage were done under a nitrogen flow in order to reduce polymer oxidation and to obtain a better thermal control. The temperature accuracy is better than 0.1 °C for the crystallization and the heat treatment temperatures. Two fibre speeds (350 and 78 μm s^{-1}) were applied by an electric motor up to the maximal displacement (18 mm). This maximal displacement is fixed to ensure that the fibre and polymer observed were in contact from the beginning of the experiment (Fig. 3). For longer distances, the fibre zone arriving in the observation zone was outside the polymer at the beginning of experiment, which implies possible artefacts. Entrance effects of the fibre into the polymer melt are not well known and are not in the scope of the mechanical model used here. Consequently, the shearing time directly depends on the fibre speed. These times were 4 min and 50 s for $V_f = 78$ μm s^{-1} and $V_f = 350$ μm s^{-1}, respectively. For each polypropylene (A, B and C) isothermal crystallizations under shear flow (at both fibre speeds) were tried at temperatures between 125 and 140 °C. When the polymer had a crystallization kinetics poorly sensitive to shear (especially A), a special procedure was applied (Fig. 2b): a pre-shearing was applied at T_c during a given time and after a waiting period, shearing was re-applied to study the crystallization. In order to assess the sensitivity of surface nucleation to previous mechanical treatment, three pre-shearing times (5, 15 and 30 s) were chosen (with either $V_f = 350$ μm s^{-1} or $V_f = 78$ μm s^{-1}) and after a fixed waiting time (1 min) a shearing was re-applied ($V_f = 78$ μm s^{-1}). Furthermore, as a reference, a static experiment was done without any fibre displacement for the three polymers at $T_c = 130$ °C (following the sample preparation described above). The basic morphologies (shape, inner structure and crystalline phase), the nucleation behavior and the growth rate usually obtained in static condition were deduced from these experiments. The growth rate of the spherulites obtained in static condition and of the cylindritic structure developed around the fibre during shearing were deduced from the measurement versus time of the spherulite radius and of the thickness of the cylindritic structure, respectively. By this method it is possible to check if the growth rate is constant or not as a function of time, (i.e., a linear increase of the radius with time or not).

8 μm-thick slices were cut out of the samples crystallized under shear. The cut was done in the plane perpendicular to the glass fibre using a ultramicrotome with a glass knife (LKB Ultrotome 4800A). The knife was often changed as the glass fibre damaged it at each cut. This sample preparation technique allows us to observe the morphologies crystallized around the fibre and to measure their thickness.

3. Results

3.1. Crystallization under static condition

For the three polypropylenes, the experiments done without any fibre displacement (i.e., in static condition) showed that no specific nucleation occurred at the fibre surface nor in its vicinity compared to the whole sample (Fig. 4). This demonstrates that the glass fibre and the sample preparation are inefficient on the nucleation compared to volume nucleation. On the opposite, Folkes and Hardwick [24] have observed an increase of the nucleation density around a PET fibre when the molecular weight of polypropylene decreases. All the growing morphologies are spherulites in the α monoclinic phase. The α-phase is the thermodynamically most stable phase and is characteristic of crystallization of polypropylene under static condition [27]. The nucleation density per unit volume is almost the same for the three polymers: 4500 ± 1000 activated nuclei per mm^3 at $T_c = 130$ °C. The growth rates of the three polymers in static condition slightly differ at $T_c = 125$ and 130 °C, as an effect of tacticity and molecular weight (Table II).

3.2. Crystallization under shear

For each polymer, there is an experimental temperature window where the polymer crystallizes under shear

TABLE II Growth rate of polypropylenes A, B, C in static condition at $T_c = 125$ and 130 °C

Polymer	Growth rate (μm s^{-1}) $T_c = 125$ °C	Growth rate (μm s^{-1}) $T_c = 130$ °C
A	—	0.1
B	0.28	0.098
C	0.29	0.09

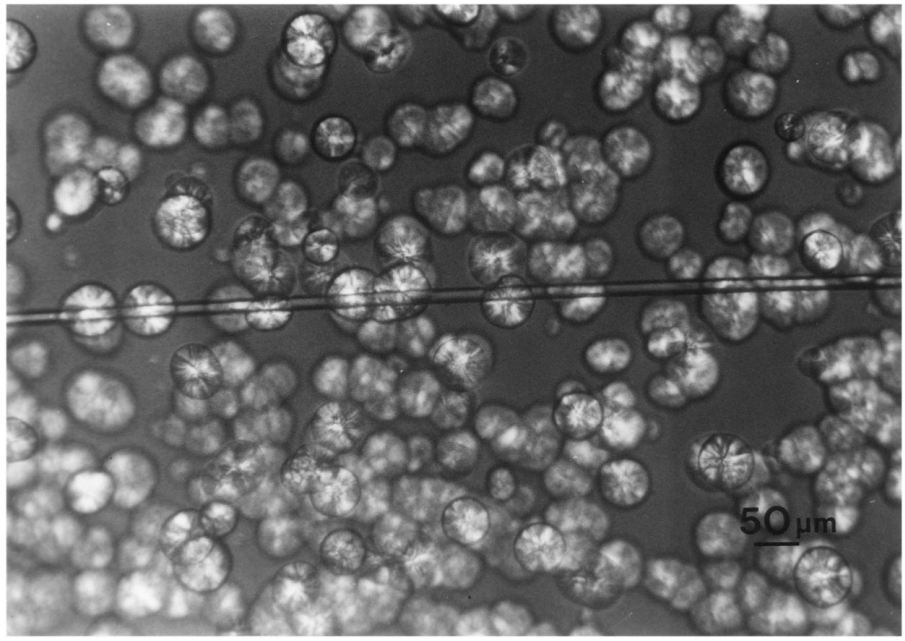

(a)

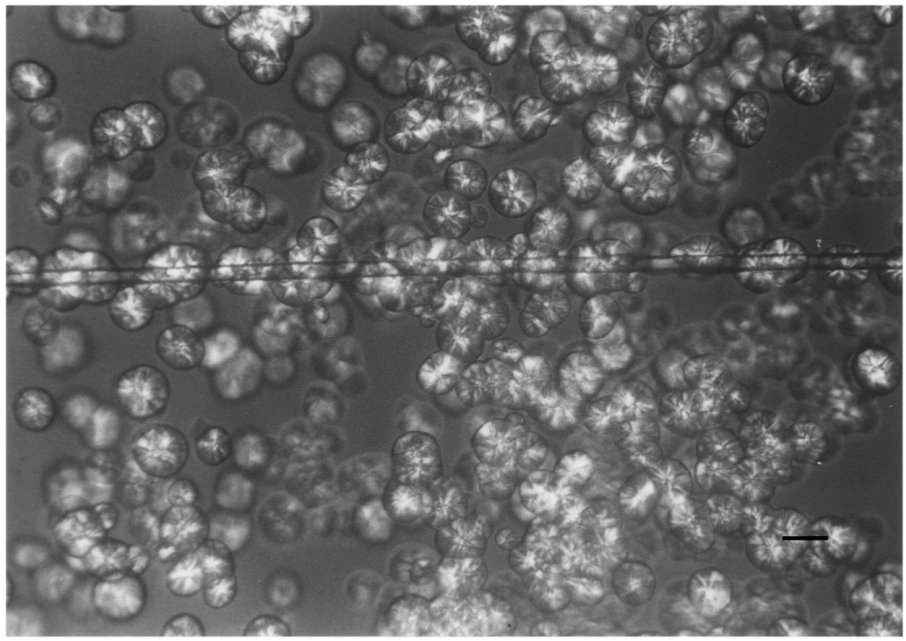

(b)

Figure 4 Crystallization of polymers A (a), B (b), C (c) at $T_c = 130\,^{\circ}C$ under static condition with the motionless glass fibre.

during the experimental time. The lower temperature boundary results from the necessity to avoid static crystallization during the cooling prior to the shear experiment and the upper limit is the temperature where crystallization cannot occur during shear. Consequently, the shear-rate and the crystallization temperature have been adapted in order to induce crystallization under shear for the three polymers. The appearance and the development of crystalline morphologies were observed during shear experiments and showed a similar behavior. All the three polymers crystallize under shear with a cylindrical morphology around the fibre. The growth rate of this morphology is constant during the shear experiment but its value depends on the polymer, temperature and fibre speed. It is very difficult to know which is the crystalline phase growing around the fibre. A more precise analysis of the crystalline phases around the glass fibre is done after crystallization on thin cuts perpendicular to the fibre direction (see below). Far from the fibre only α-phase spherulites are growing. They are identical to those formed with the same polymer at the same temperature in static condition. The main differences between all the experiments are the nucleation density at the contact with the fibre and the growth rate.

The crystallization of polypropylene C under shear was possible only for crystallization temperatures between 125 and 135 °C at both fibre speeds. A high number of nuclei appear in the volume surrounding the fibre (Fig. 5). This is specific of polymer C under shear and is not observed for other polymers in the same condition. The main phenomenon is the appearance of a high number of nuclei on the fibre surface during the fibre

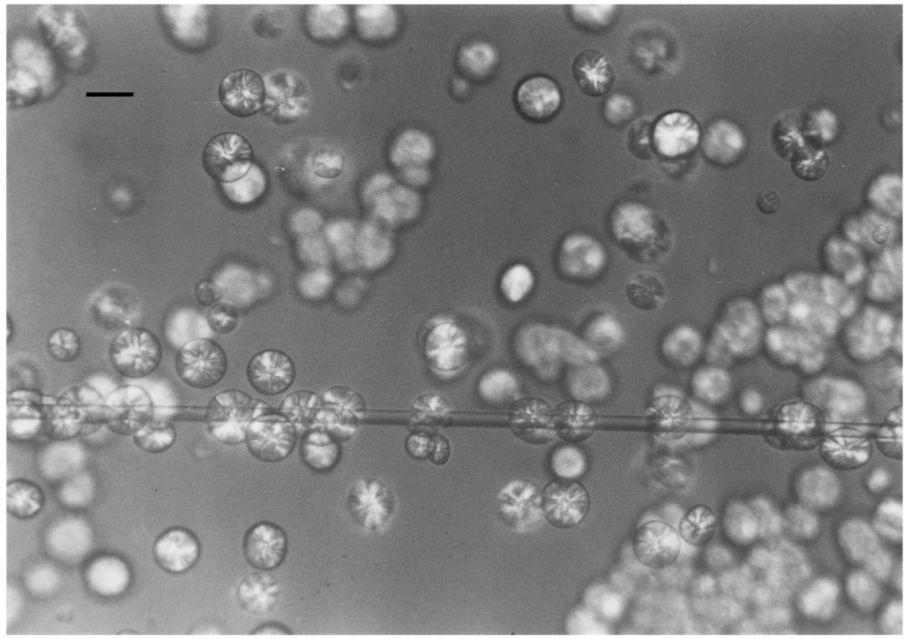

(c)

Figure 4 (*Continued*).

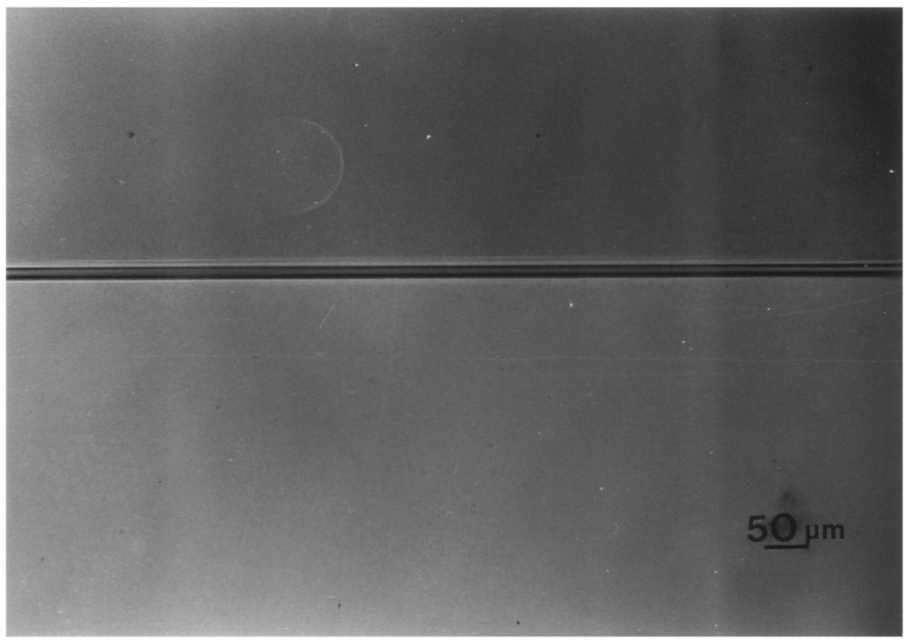

(a)

Figure 5 Crystallization under shear of polymer C at $T_c = 130\,^{\circ}\mathrm{C}$ observed at different times ($\Delta t = 20$ s between two micrographs). $V_f = 350\ \mu\mathrm{m\ s^{-1}}$.

displacement (Fig. 5). The resulting crystalline growth appears as a columnar growth of crystalline lamellae perpendicular to the fibre surface. This is due to a geometric effect because of the numerous neighboring nuclei on the fibre surface, which block any lateral growth. This radial growth is characterized by a constant rate during the whole shear experiment (Fig. 6). The maximum radius increase in these experiments is 45 μm (Fig. 6). The gap between the solid layer and the glass plate is reduced at the most from ca. 155 μm (165 μm − 8.5 μm), at the beginning of the experiment, to ca. 110 μm (165 μm − (45 μm + 8.5 μm)) at the end of the experiment. So, a large gap is kept all along the experiment, which is necessary to reduce the boundary effect of the glass plates. The growth rate depends on the velocity of the glass fibre and is much higher than the one determined in static condition at the same crystallization temperature (Fig. 7). The induction time, i.e., the beginning of crystalline growth, is obtained by the onset time in Fig. 6. It is positive as expected (the crystallization begins after the isothermal condition is reached) and almost constant for polymer C (Table III).

The nucleation and the growth rate of spherulites in the volume of polymer B around the fibre are the same under shear and in static condition. Shearing also acts on the B material but compared to C the nucleation

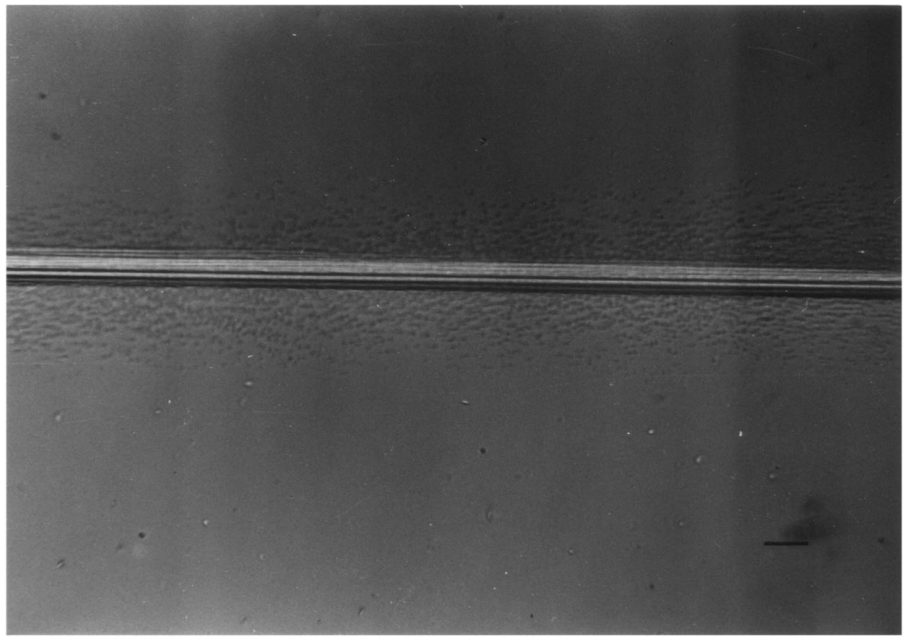

(b)

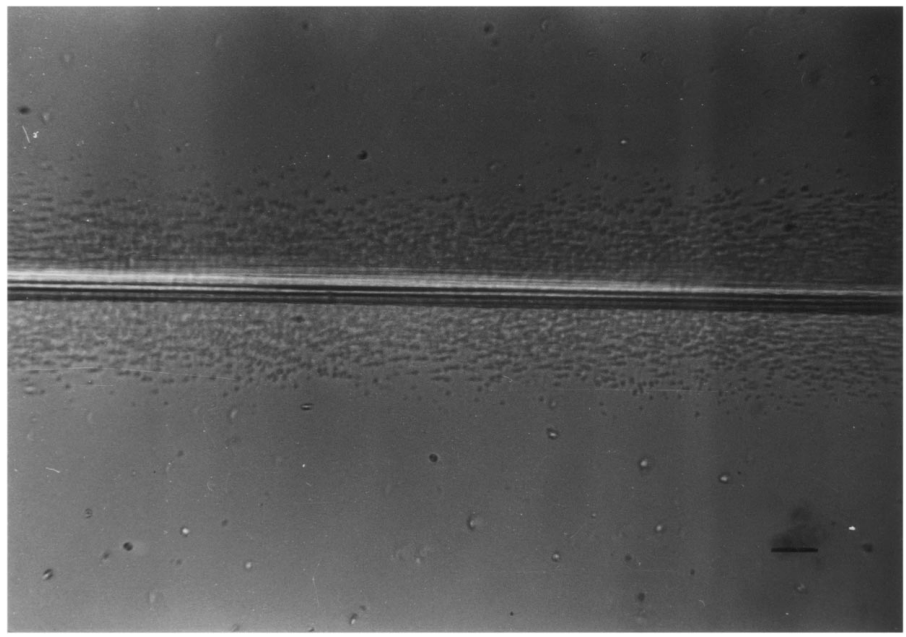

(c)

Figure 5 (*Continued*).

of the crystalline entities at the fibre surface occurred after a longer shearing time (Table III). Numerous spherulites grow from the fibre, there is a competition between the lateral growth and the nucleation of new entities. Then, for a given thermo-mechanical condition, a columnar morphology develops but with a lower final

TABLE III Induction times of polymers B and C crystallized under shear flow

Polymer	Fibre speed	$T_c = 125\,^{\circ}C$	$T_c = 130\,^{\circ}C$
B	$V_f = 78\ \mu m\ s^{-1}$	14 s	60 s
	$V_f = 350\ \mu m\ s^{-1}$	12 s	19 s
C	$V_f = 78\ \mu m\ s^{-1}$	7 s	4 s
	$V_f = 350\ \mu m\ s^{-1}$	4 s	2 s

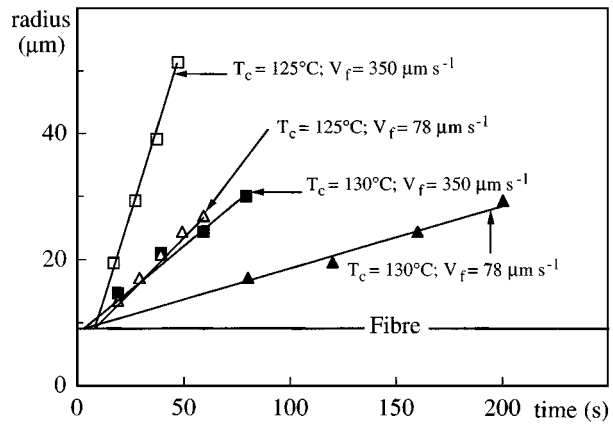

Figure 6 Evolution of the solid layer of polymer C versus time at 125 and 130 °C for both fibre speeds.

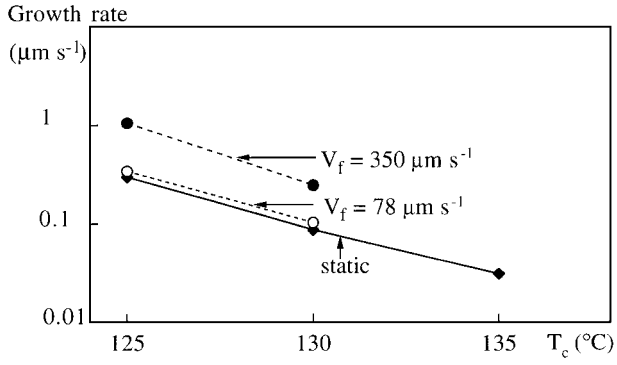

Figure 7 Growth rate measurements for polymer C as a function of crystallization temperature and fibre velocity.

thickness than for polymer C (Fig. 8a). A negligible difference of growth rates, measured at $T_c = 130\,^{\circ}$C, is observed between crystallization under shear and crystallization under static condition: $G_{\text{shear}} = 0.101\ \mu\text{m s}^{-1}$ ($V_f = 78\ \mu\text{m s}^{-1}$) and $G_{\text{static}} = 0.098\ \mu\text{m s}^{-1}$. This difference is within the experimental error. Hence, for this polymer and these experimental conditions shearing acts on nucleation but has no effect on the growth rate.

For polymer A, the shear efficiency on nucleation is very weak (Fig. 8b). Shearing has almost no nucleation effect except at $T_c = 128$ and $130\,^{\circ}$C. For these two conditions, in the same way as for polymer B, we observed the formation of a cylindrical structure around the fibre. The number of crystalline entities stuck on

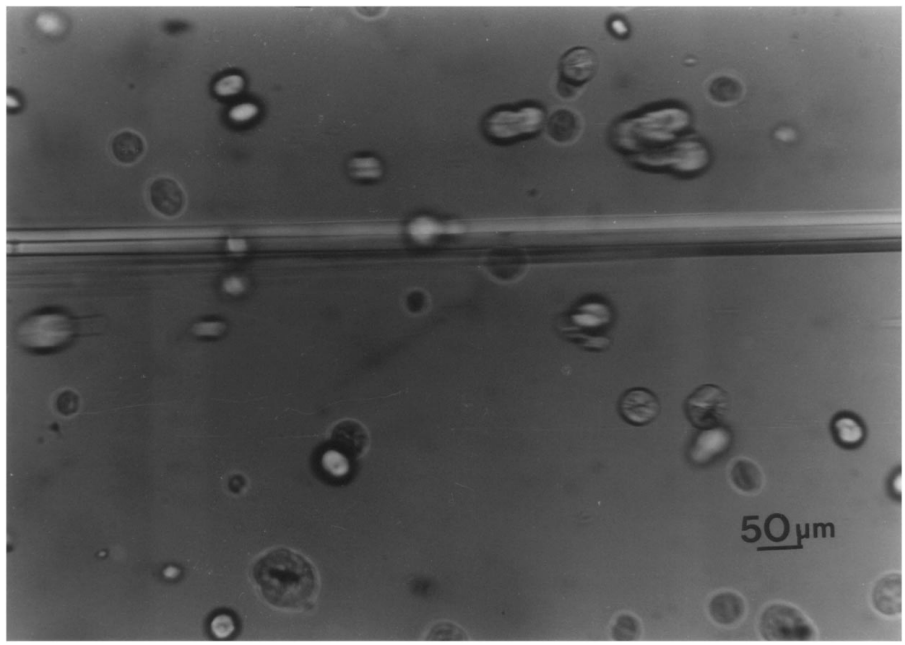

(a)

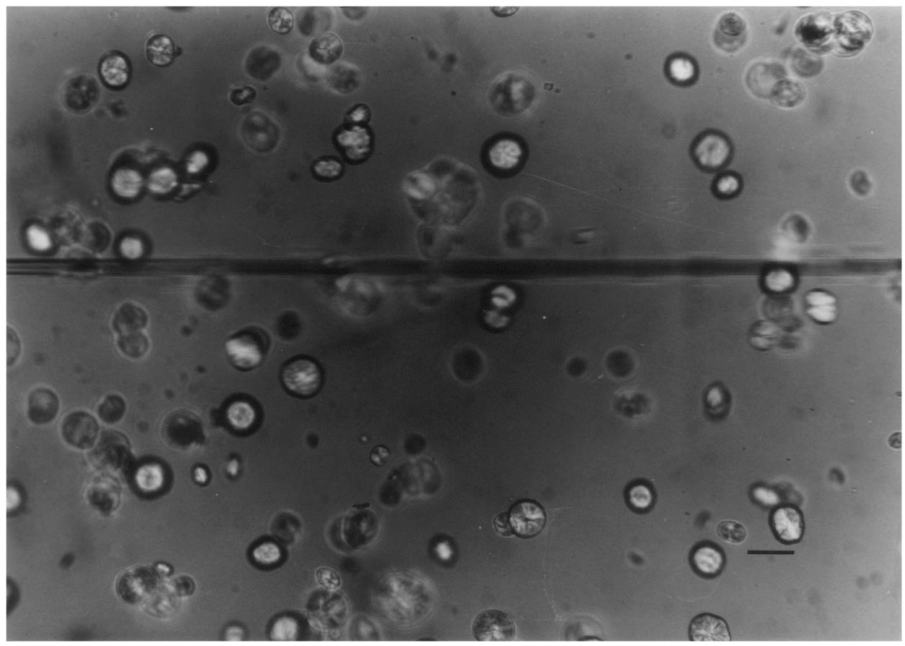

(b)

Figure 8 Crystallization under shear of polymers A and B: (a) polymer B ($T_c = 125\,^{\circ}$C, $V_f = 78\ \mu\text{m s}^{-1}$), (b) polymer A ($T_c = 128\,^{\circ}$C, $V_f = 78\ \mu\text{m s}^{-1}$) and (c) polymer A ($T_c = 130\,^{\circ}$C, $V_f = 78\ \mu\text{m s}^{-1}$), with pre-shearing.

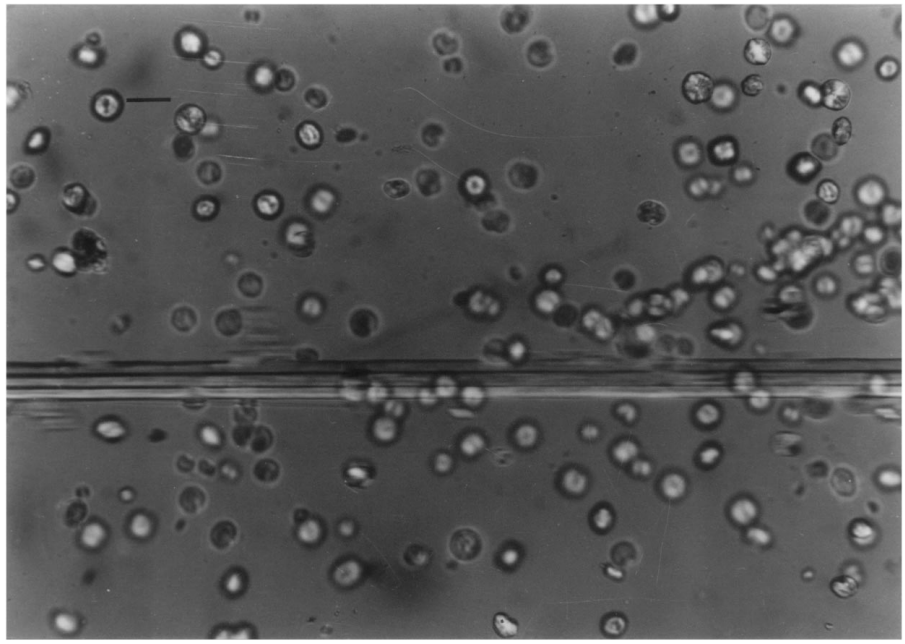

(c)

Figure 8 (*Continued*).

the fibre increased until the fibre was totally covered. A rotation of spherulites was also observed near the fibre due to the shear gradient. Shear has a very low effect on nucleation of polymer A and none on its growth rate. Hence, to study nucleation under shear and the subsequent growth, we used the special procedure described above. Six experiments were carried out at 130 °C with a pre-shearing (Fig. 8c). The major parameter of the pre-shearing is the velocity of the fibre combined with the shearing time, which act on the nucleation density at the fibre surface. For the higher speed 30 s are necessary to produce a very high number of nuclei leading to a columnar morphology, when only few nuclei appear after a 5 s pre-shearing leading to spherulites nucleated on the fibre surface. The growth rate measured under shear remains equal to the static value.

During the shear experiment, it is possible to observe the nucleation and crystalline growth and to measure the crystalline growth rate. It is also possible to define the crystalline phase of spherulites in the bulk, but not that of the cylindrical structure around the fibre. The crystalline phase (α or β) of the cylindrical structure nucleated and growing under shear must be known to allow a comparison between the growth rates under shear and in static condition. The observation of the thin cuts systematically showed α-phase with a weak positive birefringence at the contact with the fibre (Fig. 9). This α-phase ring shows a higher extension (aspect ratio about 1.5) along the thickness direction than in the median plane. The thickness of the ring depends on the polymer, temperature and fibre speed (Fig. 9). This thickness along the median plane, the plane of observation during shear experiment, is compared with the thickness formed during crystallization under shear. The latter is the product of the growth rate under shear by the crystallization time under shear, i.e., the shear time minus the induction time. Systematically, the observed and predicted thicknesses are found almost equal. Consequently, it can be concluded that polypropylene crystallizes in α-phase under shear. The growth rates of α-phase under shear and in static condition can validly be compared.

A ring of highly negatively birefringent β-phase is blocked between this first layer and the matrix of α-phase spherulites far from the fibre (Fig. 9). This β-phase was crystallized after shear under static condition. This condition seems to be sufficient to form β-phase. No β-phase spherulites were observed in purely static condition. Furthermore, polymer C presents two specific morphologies for $V_f = 350$ μm s^{-1} ($T_c = 125$ and 130 °C): numerous α-phase spherulites are formed near the fibre and two α-phase transcrystalline zones, 400 μm wide, grow from the glass slides just in front of the glass fibre (Fig. 9c and d), one of these layers containing some β-phase (Fig. 9d). The numerous spherulites result from the strong nucleation observed during shear on polymer C (Fig. 5).

Consequently, shear is highly efficient on both nucleation and growth of polymer C, whereas it acts on nucleation and not on growth of polymer B, and neither on nucleation nor on growth of polymer A. The quantitative analysis will be focused on the growth rate under shear and then specifically on polymer C, which has the highest molecular weight.

4. Discussion

The experiments were described up to now as a function of the fibre velocity. The axial movement of the fibre induces a velocity field in the polymer melt and then a shear-rate $\dot{\gamma}$. Assuming a cylindrical geometry, a sticky contact of the polymer with the fibre and the glass slides, and a power law for the polymer rheology (Equation 1), Monasse has shown [14] that the shear-rate around the fibre is equal to:

$$\dot{\gamma} = \frac{1-n}{n} \frac{1}{r^{1/n}} \left[\frac{1}{r_f^{1-1/n} - r_e^{1-1/n}} \right] V_f \qquad (2)$$

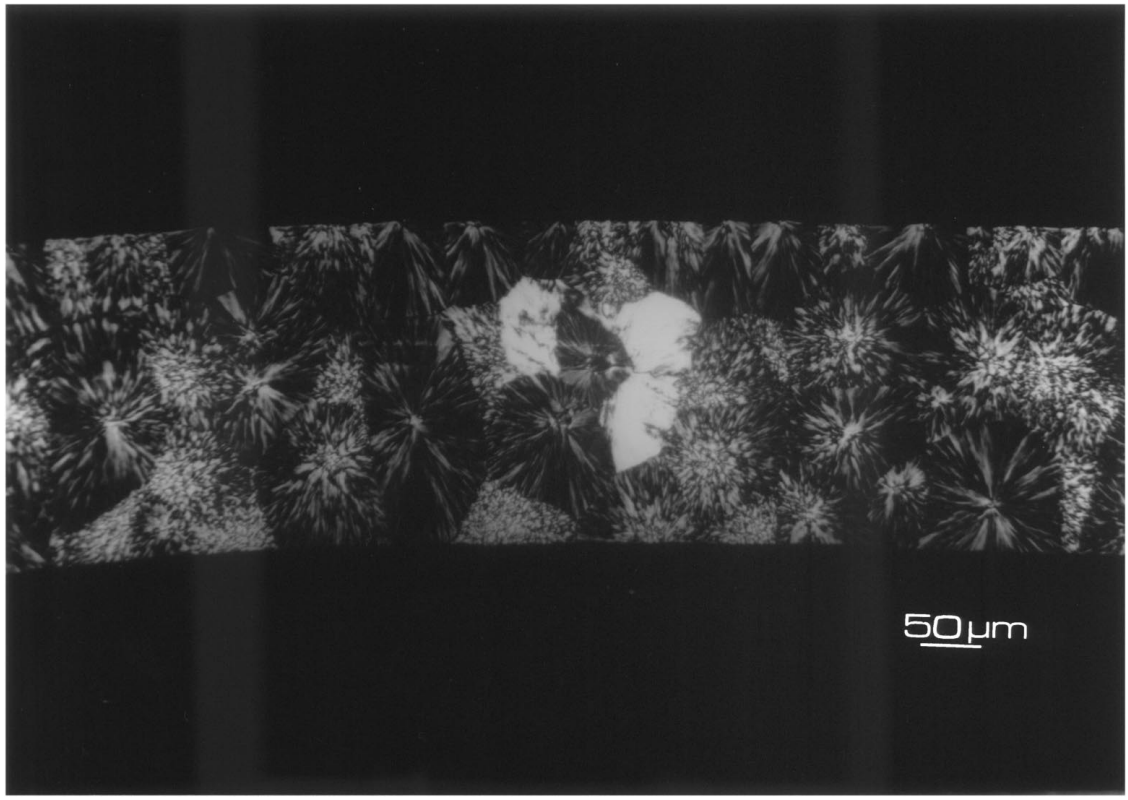

(a)

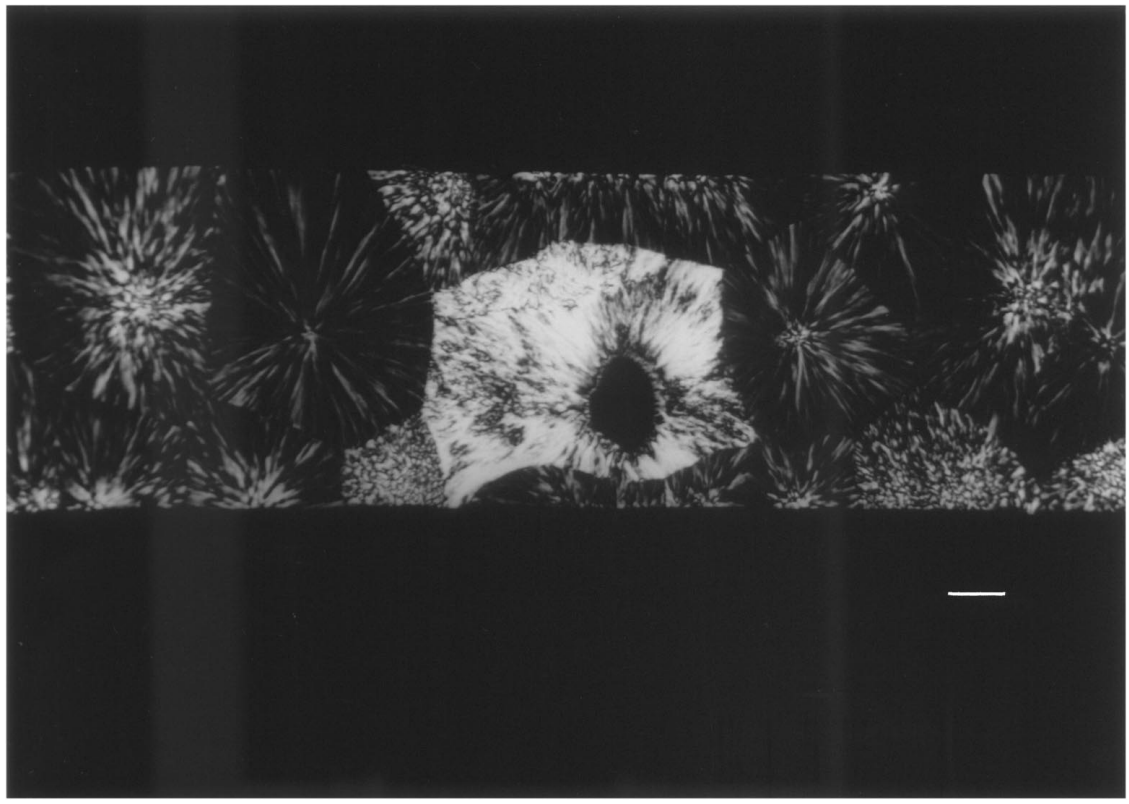

(b)

Figure 9 Morphologies around the glass fibre after crystallization under shear: (a) polymer A ($T_c = 128\,^{\circ}C$, $V_f = 350\ \mu m\ s^{-1}$), (b) polymer B ($T_c = 125\,^{\circ}C$, $V_f = 350\ \mu m\ s^{-1}$), (c) polymer C ($T_c = 125\,^{\circ}C$, $V_f = 350\ \mu m\ s^{-1}$) and (d) polymer C ($T_c = 130\,^{\circ}C$, $V_f = 350\ \mu m\ s^{-1}$).

where n is the exponent of the power law, r_f is the radius of the fibre, r_e is the half-thickness of the polymer melt ($r_e = 165\ \mu m$) and r is the distance from the fibre axis at which $\dot{\gamma}$ is calculated. The values of n were deduced from the rheological measurements (Table I).

The shear stress

$$\tau = \eta\dot{\gamma} \tag{3}$$

is then equal to

$$\tau = \frac{K}{r}\left[\left(\frac{1-n}{n}\right)V_f\frac{1}{r_f^{1-1/n} - r_e^{1-1/n}}\right]^n \tag{4}$$

where K was extrapolated to the crystallization temperature from the rheological measurements (Table I)

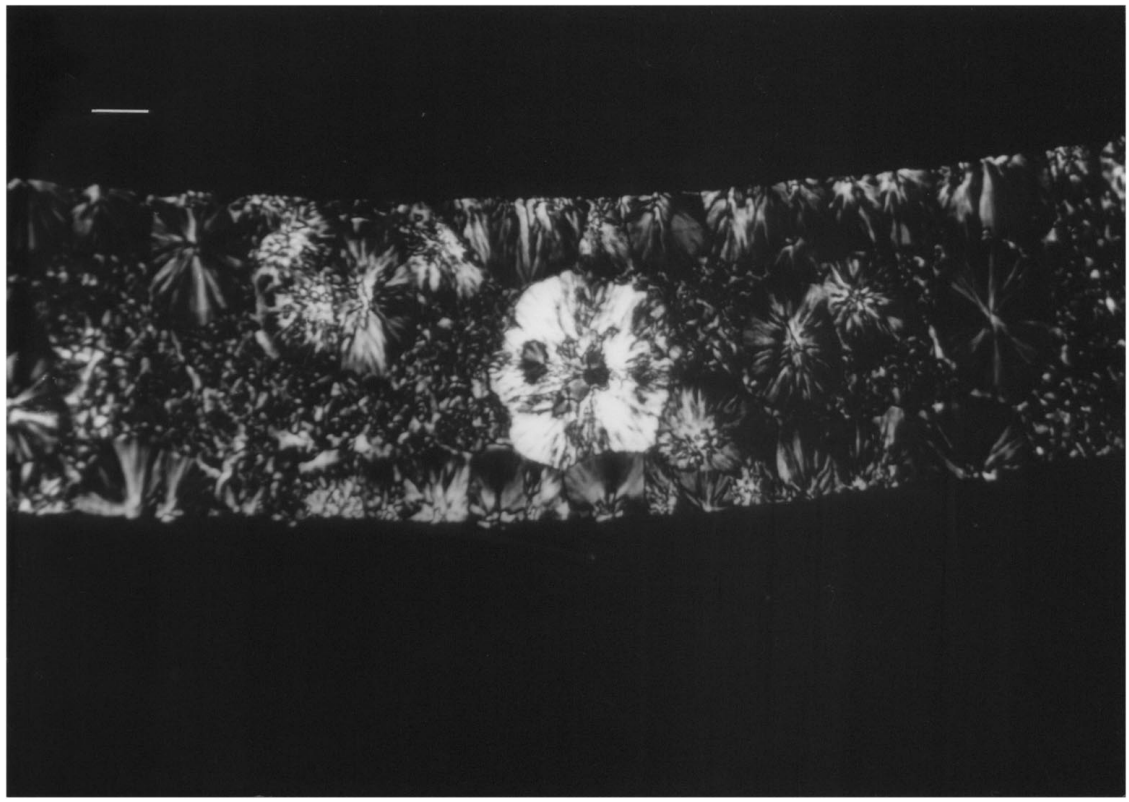

(c)

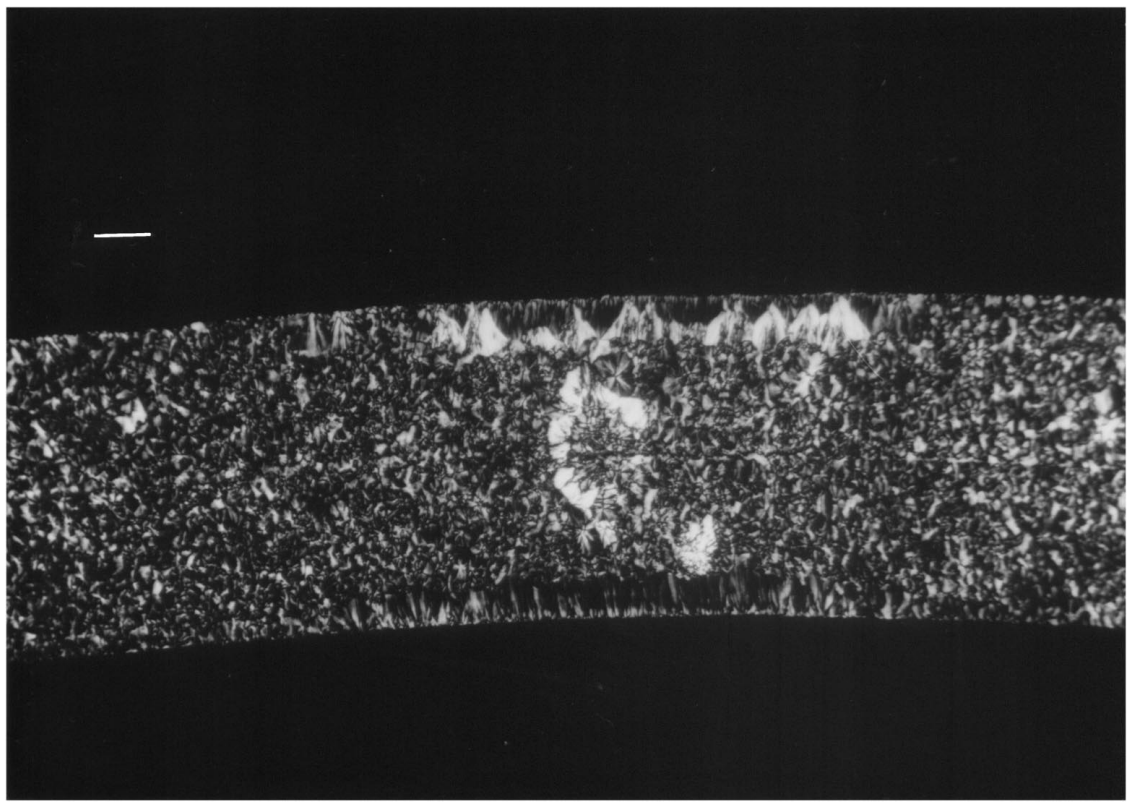

(d)

Figure 9 (*Continued*).

using an Arrhenius law. Fig. 10 shows, for the three polymers at the beginning of shear, typical variations of the shear rate $\dot{\gamma}$ and of the shear stress τ along the radius r from the fibre axis. Equations 2 and 4 can be used at the beginning of the experiment and specifically to study the nucleation process. The shear rate and the shear stress are maximum at the surface of the fibre and strongly decrease along the radius r to become very low at $r = 20$–30 μm (about 20% of the maximum value) (Fig. 10). If shear influences nucleation, the model predicts that the polymer crystallizes under shear in α-phase near the fibre (or the solid layer), at a distance up to 10–20 μm from the fibre surface, and that far from the fibre the crystallization occurs

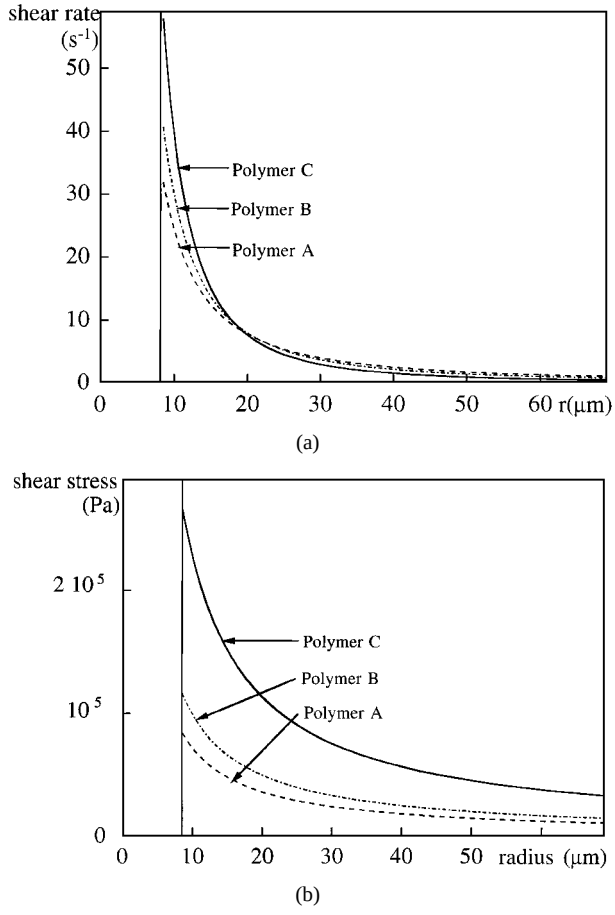

Figure 10 Evolution of the shear rate (a) and the shear stress at 130 °C (b) along the radius from the fibre axis. $V_f = 350\ \mu m\ s^{-1}$.

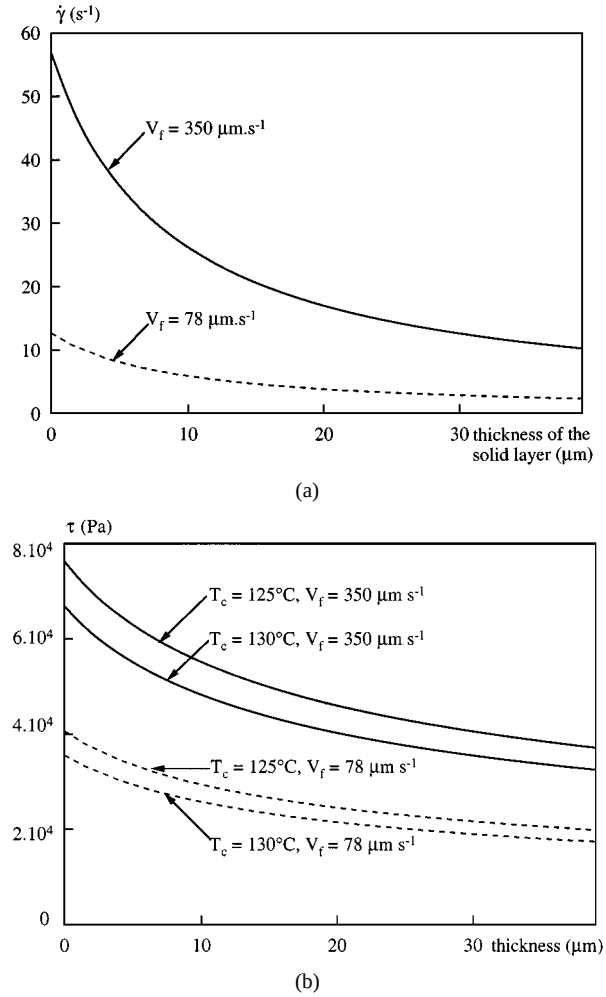

Figure 11 Evolution of the shear rate (a) and of the shear stress (b) at the crystalline growth front during the crystallization under shear. Polymer C.

in static condition. This was experimentally checked since we observed that far from the fibre the spherulites were not perturbed by the shear flow and were growing like in static condition. The shear-rate curves of the three polymers are approximately the same for a given experimental condition (Fig. 10a). It is certainly not the parameter explaining the differences of nucleation under shear observed in the three polymers. The nature of the polymer is dominant on shear stress: polymers A, B and C can be easily distinguished by increasing stress values in the shear-rate range (Fig. 10b). This effect results from the increase of viscosity with molecular weight (see Table I). This model obviously predicts a negligible effect of shearing at the surface of glass slides ($r_e = 165\ \mu m$), as observed for polymers A and B. However, it must be noticed that C presents a strong nucleation at the slide surfaces, which induces transcrystalline zones. This effect is really not explained by the model. It only proves that a very low shear-rate ($\dot{\gamma} < 0.5\ s^{-1}$) is efficient on crystallization for the polypropylene with the highest molecular weight.

The above calculation is done for $V = V_f$ at $r = r_f$, i.e., it assumes that there is no crystalline growth. This analysis is exact at the beginning of crystallization, but when the solid polymer layer expands, the condition $V = V_f$ must be applied at the boundary between solid and molten polymer (i.e., at the crystalline growth front), and no more at the fibre surface. Then, the shear rate and the shear stress at the solid/melt interface decrease according to Equations 2 and 4, respectively, where $r_{interface} = r_f + r_{solid\ layer}$ replaces r_f. A non-explicit equation is available as an effect of the kinetic law which must appear in Equations 2 and 4. The calculation is done in the median plane used for the observation under shear ($r_e = 2.5$ mm), and can also be done along the thickness direction ($r_e = 165\ \mu m$). Fig. 11 shows the evolution of the shear flow at the growth front during crystallization of polymer C at 125 and 130 °C for $V_f = 78$ and 350 $\mu m\ s^{-1}$. The values of $\dot{\gamma}$ and τ at the interface strongly decrease during the crystallization. However, the measurement of the solid layer thickness (polymers B and C) at different time intervals showed that the variation of the thickness with the shearing time was linear, leading to a constant growth rate. One would have expected a non-linear variation, as the shear rate and the shear stress at the interface decrease during the experiment (Fig. 11). Thus, the shear rate and the shear stress are too simple parameters to predict the crystallization under shear. The role of another important mechanical parameter, the shear strain, will be examined below.

Two main assumptions are made to build our mechanical model: a power-law rheology around the glass fibre and a cylindrical symmetry. These assumptions are based on the strong localization of the shear-rate very

near the glass fibre or at the boundary between solid and liquid polymer. Fig. 10a shows that the shear-rate around the fibre is larger than 35 s^{-1} at the beginning of the experiment. Fig. 1 proves that a power law is a good approximation for the three polymers in this range of shear-rate. The shear-rate strongly decreases along the radius and at a distance of about 10 μm the rheology is no more compatible with a power law. Nevertheless, this does not really affect the value of the shear-rate at the solid/liquid interface, as demonstrated by numerical calculations using Carreau's law [28], which better describes the rheological behaviour. It is the reason why this assumption, which allows analytical developments, is kept. Concerning the cylindrical geometry, the presence of glass plates questions this second assumption. The high value of the shear-rate at the boundary of the solid layer is quite insensitive to the location of the outside boundary as soon as the distance between them is sufficient ($r_e - r_{interface} > 50$ μm). An analysis of parameters sensitivity of Equation 2 shows that the shear-rate slowly decreases when the radius $r_{interface}$ increases in a short range. If the radius $r_{interface}$ tends to the external radius r_e, Equation 2 now predicts a strong increase of the shear-rate. Consequently, it is necessary to limit the variation of $r_{interface}$ with respect to r_e. That is why a thick medium is used ($e = 330$ μm) in order to maintain a large gap all along the experiment and to avoid a too large perturbation of the shear-rate by the glass plates. In that condition, we observe that the shear-rate at the solid-liquid interface remains almost constant around the interface and the cylindrical symmetry, from a mechanical aspect, is fairly respected. According to Campbell and White [25] the hypothesis of residual stresses must be rejected, the crystallization being highly localized around the fibre in a thick sample.

The shear strain can be calculated during the crystallization. It is the cumulated shear strain at a point, from the beginning of shear up to the moment the growth front passes over this point. The calculation can be done at various radii in the median plane by integration of the shear-rate during all the time the polymer remains molten. This parameter may be pertinent to analyze the growth rate dependence on shear for polymer C. It can be noticed that the polymer which first crystallized under shear was located near the fibre and was subjected to a high shear-rate but for a short time. On the contrary, the polymer crystallizing under shear far from the fibre experienced at the beginning a low shear-rate but this quantity gradually increased when the growth front moved. Finally, the shear strain remains almost constant except for the shortest times (Fig. 12). This analysis can be extended to other experimental conditions: the shear strain increases up to an asymptotical value which depends on temperature and fibre speed. The calculation can also be done in the thickness direction. An asymptotical value 10% higher than in the median plane is predicted. In the same way, a larger extension of the α-phase layer in the thickness than in the median plane (about 50% higher) was systematically observed on thin sections (Fig. 9). The general trend is exact but the amplitude of the effect is

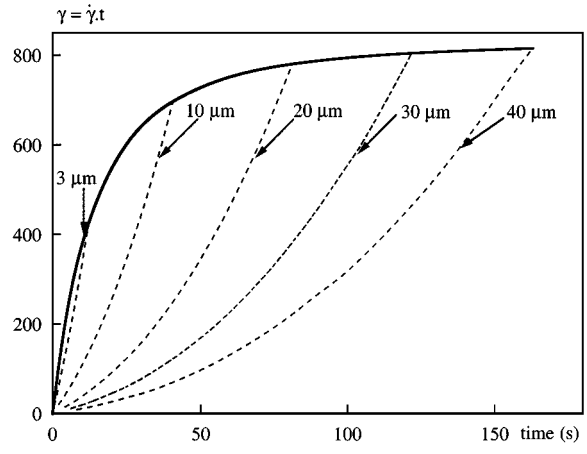

Figure 12 Evolution of the shear strain at different distances from the fibre surface between the beginning of the experiment and the polymer solidification (dashed lines). The solid curve corresponds to the strain at the growth front. Polymer C, $T_c = 130\,^{\circ}C$, $V_f = 350$ μm s^{-1}.

larger than expected. It can also be noticed that the transition time up to the asymptote is very close to the induction time given in Table III. A similar treatment was proposed by Janeschitz-Kriegl and co-workers to model the overall kinetics after a short-term shearing inside a duct in isothermal condition [22, 26]. The model mainly considers the length of thread-like precursors of crystallization, which is found proportional to $\dot{\gamma}^4 t_s^2 = \gamma^2 \dot{\gamma}^2$, where t_s, $\dot{\gamma}$ and γ are the shearing time, the critical shear-rate and shear, respectively. During our experiments the analysis of crystalline growth rate was privileged and we found a large effect of shear on the growth rate.

Only the α-phase crystallizes under shear in these experimental conditions. The growth rates of the α-phase under shear G_{sh} and in static condition G_{st} can be compared at the same temperature. We define the shear factor for the growth rate as $S = G_{sh}/G_{st}$. The growth rates in static conditions are: $G\,(125\,^{\circ}C) = 0.29$ μm s^{-1} and $G\,(130\,^{\circ}C) = 0.09$ μm s^{-1}. The analysis of the shear factor as a function of the shear strain is a way to compare experiments under shear (Fig. 13). A low fibre speed ($V = 78$ μm s^{-1}) induces a weak

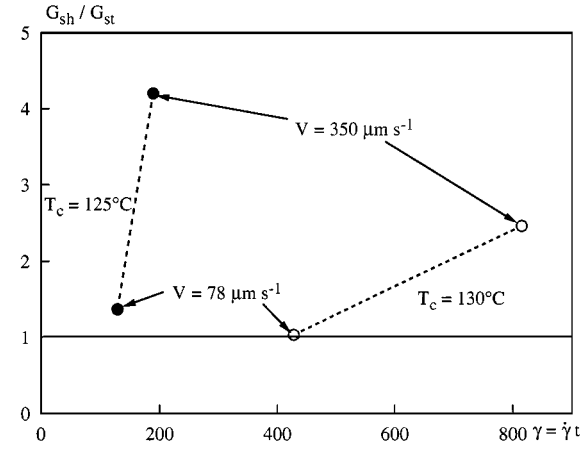

Figure 13 Effect of the shear strain on the enhancement of crystalline growth under shear, as characterized by the ratio of the growth rates under shear G_{sh} and in static condition G_{st}, Polymer C.

increase of the growth rate for both temperatures. A higher fibre speed leads to a strong increase of the growth rate, higher at 125 °C than at 130 °C. A slower shear strain is necessary at 125 °C to induce the crystalline growth, which explains the efficiency of shear at the lower temperature. The thickness of the α-phase layer results only from the product of the growth rate by the effective shearing time, i.e., the shearing time minus the induction time. The β-phase appears just after the end of shearing, which corresponds to a limited area, the rest of the sample containing no β-phase at all except for a small amount in some transcrystalline regions (Fig. 9). This result must be emphasized, because previous papers have drawn attention to the promoting effect of shear stress on the formation of β-modification [16, 19, 29]. Some investigations, mainly by the fibre pulling technique, have defined the thermal and mechanical conditions of formation of β-phase more exactly [16, 18, 20, 30]. It seems that the β-phase observed in our experiments results from a α-to-β transformation during the crystal growth after the shearing, i.e., during the relaxation of the orientation. Such a α-to-β transition was recently described by Varga and Karger-Kocsis [20], but not coupled with a mechanical analysis of the flow pattern. Lovinger *et al*. [31] have also observed the α-to-β transformation during experiments in a large thermal gradient.

We have used here rheological parameters deduced from high temperature dynamic measurements. The extrapolation to very low temperatures and the use of simple shear flow can be questionable. The fluid rheology is extrapolated to a temperature range where crystallization appears, i.e., to a zone of rheological change from a fluid to a solid. The analysis of the rheological change during the transition is a formidable task, beyond the scope of the present paper. With the geometry used, the principal and amazing aspect is the displacement of a sharp growth front which separates the semi-crystalline solid from the still molten polymer. From a mechanical point of view, the growth front is considered as an expanding tool. This mechanical approximation is not so bad. Furthermore, if on a macroscopic scale the polymer undergoes a shear flow, at a microscopic level the deposit of a chain segment on the surface of the solid layer can lead to a local elongational flow. One knows that such a flow is much more efficient on crystallization than shear [32]. This effect could explain the important nucleation of polymer C on the glass surface in front of the glass fibre (Fig. 9c and d). Then, although the polymer crystallizes in a shear flow, it is not sure that at the molecular level shear is the main mechanical parameter.

5. Conclusion

The shear flow induced by the displacement of a glass fibre deeply modifies the nucleation and growth of isotactic polypropylene. The nucleation and the growth under shear concern only the α-phase. The sensitivity of a given polypropylene to shear depends on its molecular weight. The higher the molecular weight, the more enhanced the nucleation and then the growth rate. A high molecular weight and a significant shear are necessary to observe an increase of the growth rate, which may be more than three times the static value. β-phase develops after shear in a region previously subjected to a noticeable shear. α-phase grows at a constant rate under a non-constant shear-rate. Therefore, the shear rate and the shear stress are too simple parameters to describe the crystalline growth under shear. The shear strain is able to explain the crystalline growth under shear in an isothermal condition.

Acknowledgements

The European Community must be acknowledged for the financial support of this work as a part of the Brite-Euram cooperative program (Prospero) no. BRE2.CT92.0331.

References

1. T. W. HAAS and B. MAXWELL, *Polym. Eng. Sci*. **9** (1969) 225.
2. A. WERETA and C. GOGOS, *ibid.* **11** (1971) 19.
3. R. R. LAGASSE and B. MAXWELL, *ibid.* **16** (1976) 189.
4. B. MONASSE, *J. Mater. Sci*. **30** (1995) 5002.
5. C. TRIBOUT, B. MONASSE and J. M. HAUDIN, *Colloid Polym. Sci.* **274** (1996) 197.
6. K. KOBAYASHI and T. NAGASAWA, *J. Macromol. Sci. Phys. B* **4(2)** (1970) 331.
7. D. KRUEGER and G. S. Y. YEH, *J. Appl. Phys.* **43** (1972) 4339.
8. A. K. FRITZSCHE and F. P. PRICE, *Polym. Eng. Sci*. **14** (1974) 401.
9. A. K. FRITZSCHE, F. P. PRICE and R. D. ULRICH, *ibid.* **16** (1976) 182.
10. P. G. ANDERSEN and S. H. CARR, *ibid.* **18** (1978) 215.
11. C. H. SHERWOOD, F. P. PRICE and R. S. STEIN, *J. Polym. Sci. Polym. Symp*. **63** (1978) 77.
12. M. D. WOLKOWICZ, *ibid.* **63** (1978) 365.
13. V. TAN and C. GOGOS, *Polym. Eng. Sci*. **16** (1976) 512.
14. B. MONASSE, *J. Mater. Sci*. **27** (1992) 6047.
15. Å. LARSEN and B. MONASSE, in Eighth Annual Meeting of the Polymer Processing Society (New Delhi, 1992) pp. 6–17.
16. E. DEVAUX and B. CHABERT, *Polym. Comm*. **32** (1991) 464.
17. B. CHABERT and J. CHAUCHARD, *Ann. Chim. Fr*. **16** (1991) 173.
18. J. L. THOMASON and A. A. VAN ROOYEN, *J. Mater. Sci.* **27** (1992) 897.
19. J. VARGA and J. KARGER-KOCSIS, *Composites Sci. Technol*. **48** (1993) 191.
20. *Idem., J. Polym. Sci. Polym. Phys. Ed*. **34** (1996) 657.
21. A. MISRA, B. DEOPURA, S. F. XAVIER, F. D. HARTLEY and R. H. PETERS, *Angew. Makromol. Chem.* **113** (1983) 113.
22. S. LIEDAUER, G. EDER, H. JANESCHITZ-KRIEGL, P. JERSCHOW, W. GEYMAYER and E. INGOLIC, *Intern. Polym. Processing* **8** (1993) 236.
23. D. CAMPBELL and M. M. QAYYUM, *J. Polym. Sci. Polym. Phys. Ed*. **18** (1980) 83.
24. M. J. FOLKES and S. T. HARDWICK, *J. Mater. Sci. Lett*. **3** (1984) 1071.
25. D. CAMPBELL and J. R. WHITE, *Angew. Makromol. Chem.* **122** (1984) 61.
26. H. JANESCHITZ-KRIEGL, E. FLEISCHMANN and W. GEYMAYER, in "Polypropylene: Structure, Blends and Composites," Vol. 1, edited by J. Karger-Kocsis (Chapman & Hall, London, 1995) p. 295.
27. G. NATTA and P. CORRADINI, *Nuovo Cimento Suppl*. **15** (1960) 40.
28. P. J. CARREAU, *Trans. Soc. Rheology* **16** (1972) 99.

29. H. J. LEUGERING and G. KIRSCH, *Angew. Makromol. Chem.* **33** (1973) 17.
30. J. VARGA, in "Polypropylene: Structure, Blends and Composites," Vol. 1, edited by J. Karger-Kocsis (Chapman & Hall, London, 1995) p. 56.
31. A. J. LOVINGER, J.O. CHUA and C. C. GRYTE, *J. Polym. Sci. Polym. Phys. Ed.* **15** (1977) 641.
32. M. R. MACKLEY and A. KELLER, *Phil. Trans. Roy. Soc. (London), Vol. 278* **A 1276** (1975) 29.

Received 19 August
and accepted 12 November 1998